Strangeness enhancement in $p+A$ and S+A interactions at energies near 200A GeV

V. Topor Pop*
Department of Physics, Columbia University, New York, New York 10027
and Dipartimento di Fisica "G. Galilei," Via Marzolo 8-35131, Padova, Italy

M. Gyulassy
Department of Physics, Columbia University, New York, New York 10027

X.N. Wang
Nuclear Science Division, Lawrence Berkeley Laboratory, University of California, Berkeley, California 94720

A. Andrighetto, M. Morando, F. Pellegrini, R.A. Ricci, and G. Segato
Dipartimento di Fisica "G. Galilei," Via Marzolo 8-35131, Padova, Italy
and INFN Sezione di Padova, Padova, Italy
(Received 27 March 1995)

The systematics of strangeness enhancement is calculated using the HIJING and VENUS models and compared to recent data on pp, pA, and AA collisions at CERN/SPS energies (200A GeV). The HIJING model is used to perform a *linear* extrapolation from pp to AA. VENUS is used to estimate the effects of final state cascading and possible nonconventional production mechanisms. This comparison shows that the large enhancement of strangeness observed in S+Au collisions, interpreted previously as possible evidence for quark-gluon plasma formation, has its origins in nonequilibrium dynamics of few nucleon systems. A factor of 2 enhancement of Λ^0 at midrapidity is indicated by recent pS data, where on the average *one* projectile nucleon interacts with only two target nucleons. There appears to be another factor of 2 enhancement in the light ion reaction SS relative to pS, when on the average only two projectile nucleons interact with two target ones.

PACS number(s): 25.75.+r, 24.10.Jv, 24.85.+p, 25.40.Ve

I. INTRODUCTION

The search for new states of dense nuclear matter is one of the most active areas of research in nuclear physics [1,2]. Enhanced strangeness production in ultrarelativistic heavy ion collisions was suggested long ago [3] as a signal for quark-gluon plasma formation [4–6], and has been observed at both the Alternating Gradient Synchrotron (AGS) and Super Proton Synchrotron (SPS). There are extensive data from both the SPS at CERN [7–38] and the AGS at BNL [39–45] on strangeness yields from reactions ranging from elementary $p+p$ to $p+A_T$ and A_B+A_T for targets ranging up to $A_T \approx 200$ and beams up to $A_B=30$. Detailed rapidity and transverse momentum spectra of $(K^+,K^-,K_s^0,\Lambda,\bar{\Lambda})$ are available and spectra of Ξ^- and even Ω^- are becoming available. In all cases their yield relative to pions or negative hadrons is larger in nucleus-nucleus collisions than expected from geometrically scaled proton-proton collisions. New experiments with truly heavy ion projectiles are in progress with Au beams at BNL [46,47] and with Pb beams at CERN [Pb(170A GeV)+Pb] [6] and will soon extend the data base considerably.

These and other data on nuclear reactions have stimulated the development of many hadronic transport models to address the problem of multiparticle production in nuclear collisions. These include dual partons models (DPM's) [48–54], quark-gluon string models (QGSM's) [55–59], VENUS [60], FRITIOF [61,62], ATTILA [63], HIJING [64–68], and RQMD models [69–74], parton string model (PSM) [75], HIJET [76], and the parton cascade model (PCM) [77–79]. An excellent review and detailed comparison of the models is given by Werner in Ref. [60].

At present no conventional explanation of the large enhancement of hyperons or antihyperons has been found. The Pomeron exchange picture has motivated the development of many of the above models with the Pomeron modeled in terms of colored strings. However, the string picture itself suggests the possibility of new dynamical mechanisms ranging from string fusion to color rope formation. Some of the above transport models like RQMD [74] and VENUS [60] include such non-conventional mechanisms as default options. These proposed novel *nonequilibrium* dynamical mechanisms were shown to be able to reproduce many features of the observed strangeness enhancement [80–82,72,73,60]. On the other hand, there have been many attempts (see, e.g., the review by Heinz in [1], p. 205c, and references therein) to attribute the strangeness enhancement to the formation of an equilibrated fireball containing a quark-gluon plasma state [1,5].

Therefore it appears that either nonconventional multiparticle mechanisms or the existence of a new form of matter seems to be indicated by the observed strangeness enhancement. Either case is of basic interest. The goal of the present study is to clarify which of these alternatives is more compelling. We use the HIJING model [64–68] to perform a *lin-*

*On leave of absence from Institute for Space Sciences, P.O. Box MG-6, Bucharest, Romania; Electronic address: TOPOR@ROIFA.BITNET(EARN), TOPOR@PADOVA.INFN.IT

ear extrapolation of strangeness production dynamics from pp to AA taking into account essential nuclear geometry and kinematical constraints. At higher collider energies it includes perturbative QCD (PQCD) semihard processes, but in the SPS range it reduces essentially to a hybrid version of the FRITIOF and DPM models. We use the VENUS model [60] to estimate possible effects of final state cascading and new mechanisms of strangeness production in few nucleon processes. The nonconventional mechanism in VENUS4.13 is the occurrence of "double strings" which may form when one projectile nucleon interacts with two or more target nucleons. A double string is defined as a color singlet baryon configuration consisting of one projectile quark connected to two different valence quarks in the target via a three gluon vertex. In earlier versions of the model the parametrization of the vertex kinematics led to anomalously large baryon stopping power. In the present version, the double string phenomenology is constrained to reproduce the $pA \rightarrow pX$ data. However, the new feature, see Eq. (15.52) in Ref. [60], is the assumption that the probability for hyperon production in the fragmentation regions is enhanced by a factor of 2 relative to the single string rates. This enhanced strangeness production mechanism due to double strings is similar to that postulated in the color rope model [83] and incorporated into the RQMD model. The hyperon enhancement in VENUS is, however, more confined to the fragmentation regions.

Both HIJING and VENUS models have been compared to a wide variety of data in pp, pA, and AA collisions [66,67,60]. However, no systematic study of strangeness production at SPS CERN energies has been performed up to now. In addition, there have been substantial changes in the final published data [18] relative to earlier comparisons to preliminary data [7,8]. In this paper, we calculate the rapidity and transverse momentum spectra of strange particles for pp, minimum bias collisions of pS, pAg, and pAu, and central collisions of S+S, Ag, Au, W, at the energy of 200A GeV and Pb+Pb at the energy of 170A GeV. We focus special emphasis on the comparison with the data on pp, pS, and SS from Alber *et al.* [18]. That comparison reveals that much of the enhancement of strangeness in heavy ion collisions can be traced back to the enhancement of strangeness in the lightest nontrivial ion collisions, $p+$S. Our main conclusion based on these data is that the enhancement of strangeness observed in S+Au is therefore most likely due to new nonequilibrium multiparticle production mechanisms in processes involving *few* nucleon systems.

This paper is organized as follows. A brief description of the HIJING Monte Carlo model and theoretical background are given in Sec. II. For a detailed discussion of the VENUS model, we refer to the review in [60]. In Sec. III, detailed numerical results with HIJING and VENUS for pp, pA, and AA reactions at CERN SPS energies ($\sqrt{s} \simeq 20A$ GeV) for strangeness production are compared to experimental data and other model predictions. Section IV concludes with a summary and discussion of results.

II. OUTLINE OF THE HIJING MODEL

A detailed discussion of the HIJING Monte Carlo model was reported in Refs. [64–68]. The formulation of HIJING was guided by the LUND FRITIOF and dual parton model (DPM) phenomenology for soft nucleus-nucleus reactions at intermediate energies ($\sqrt{s}<20$ GeV) and implementation of perturbative QCD (PQCD) processes in the PYTHIA model [84] for hadronic interactions. We give in this section a brief review of the aspects of the model relevant to hadronic interaction.

(1) Exact diffuse nuclear geometry is used to calculate the impact parameter dependence of the number of inelastic processes [63].

(2) Soft beam jets are modeled by quark-diquark strings with gluon kinks along the lines of the DPM and FRITIOF models. Multiple low p_T exchanges among the end point constituents are included.

(3) The model includes multiple minijet production with initial and final state radiation along the lines of the PYTHIA model and with cross sections calculated within the eikonal formalism.

(4) Hadronization is performed via the JETSET7.2 algorithm [84] that summarizes data on e^+e^-.

(5) HIJING does not incorporate any mechanism for final state interactions among low p_T produced particles nor does it have color rope formation.

The rate of multiple minijet production in HIJING is constrained by the cross sections in nucleon-nucleon collision. Within an eikonal formalism [85] the total elastic cross sections $\sigma_{\rm el}$, total inelastic cross sections $\sigma_{\rm in}$, and total cross sections $\sigma_{\rm tot}$ can be expressed as:

$$\sigma_{\rm el}=\pi\int_0^\infty db^2\{1-\exp[-\chi(b,s)]\}^2, \tag{1}$$

$$\sigma_{\rm in}=\pi\int_0^\infty db^2\{1-\exp[-2\chi(b,s)]\}, \tag{2}$$

$$\sigma_{\rm tot}=2\pi\int_0^\infty db^2\{1-\exp[-\chi(b,s)]\}. \tag{3}$$

Strong interactions involved in hadronic collisions can be generally divided into two categories depending on the scale of momentum transfer q^2 of the processes. If $q^2<\Lambda^2_{\rm QCD}$ the collisions are nonperturbative and considered *soft* and modeled by beam jet fragmentation via the string model. If $q^2 \gg \Lambda^2_{\rm QCD}$ the subprocesses on the parton level are considered *hard* and calculated via PQCD [67].

In the limit that the real part of the scattering amplitude is small and the eikonal function $\chi(b,s)$ is real, the factor

$$g(b,s)=1-\exp[-2\chi(b,s)] \tag{4}$$

can be interpreted in terms of a semiclassical probabilistic model as *the probability for an inelastic event of nucleon-nucleon collisions at impact parameter b* which may be caused by hard, semihard, or soft parton interactions.

To calculate the probability of multiple minijets, the main dynamical assumption is that they are independent. This holds as long as their average number is not too large as is the case below Large Hadron Collider (LHC) energies [67]. When shadowing can be neglected, the probability of no jets and j independent jet production in an inelastic event at impact parameter b, can be written as

$$g_0(b,s)=\{1-\exp[-2\chi_s(b,s)]\}\exp[-2\chi_h(b,s)], \quad (5)$$

$$g_j(b,s)=\frac{[2\chi_h(b,s)]^j}{j!}\exp[-2\chi_h(b,s)], \quad j\geq 1, \quad (6)$$

where $\chi_s(b,s)$ is the eikonal function for soft interaction, $2\chi_h(b,s)$ is the average number of hard parton interactions at a given impact parameter, and $\exp[-2\chi_s(b,s)]$ is the probability for no soft interaction. Summing Eqs. (5) and (6) over all values of j leads to

$$\sum_{j=0}^{\infty} g_j(b,s)=1-\exp[-2\chi_s(b,s)-2\chi_h(b,s)]. \quad (7)$$

Comparing with Eq. (4) one has

$$\chi(b,s)=\chi_s(b,s)+\chi_h(b,s). \quad (8)$$

Assuming that the parton distribution function is factorizable in longitudinal and transverse directions and that the shadowing can be neglected the average number of hard interactions $2\chi_h(b,s)$ at the impact parameter b is given by

$$\chi_h(b,s)=\frac{1}{2}\sigma_{\rm jet}(s)T_N(b,s), \quad (9)$$

where $T_N(b,s)$ is the effective partonic overlap function of the nucleons at impact parameter b.

$$T_N(b,s)=\int d^2b'\rho(b')\rho(|b-b'|) \quad (10)$$

with normalization $\int d^2bT_N(b,s)=1$, and $\sigma_{\rm jet}$ is the PQCD cross section of parton interaction or jet production [66,67]. Note that $\xi=b/b_0(s)$, where $b_0(s)$ provides a measure of the geometrical size of the nucleon $\pi b_0^2(s)=\sigma_s(s)/2$ assuming the same geometrical distribution for both soft and hard overlap functions,

$$\chi_s(\xi,s)\equiv\frac{\sigma_s}{2\sigma_0}\chi_0(\xi), \quad (11)$$

$$\chi_h(\xi,s)\equiv\frac{\sigma_{\rm jet}}{2\sigma_0(s)}\chi_0(\xi), \quad (12)$$

$$\chi(\xi,s)\equiv\frac{1}{2\sigma_0}[\sigma_s(s)+\sigma_{\rm jet}(s)]\chi_0(\xi). \quad (13)$$

We note that $\chi(\xi,s)$ is a function not only of ξ but also of $\sqrt{s}$ because of the $\sqrt{s}$ dependence on the jet cross section $\sigma_{\rm jet}(s)$. Geometrical scaling implies on the other hand that $\chi_s(\xi,s)=\chi_0(\xi)$ is only a function of ξ. Therefore geometrical scaling is broken at high energies by the introduction of $\sigma_{\rm jet}(s)$ of jet production.

The cross sections of nucleon-nucleon collisions can in this case be expressed as

$$\sigma_{\rm el}=\sigma_0(s)\int_0^{\infty} d\xi^2\{1-\exp[-\chi(\xi,s)]\}^2, \quad (14)$$

$$\sigma_{\rm in}=\sigma_0(s)\int_0^{\infty} d\xi^2\{1-\exp[-2\chi(\xi,s)]\}, \quad (15)$$

$$\sigma_{\rm tot}=2\sigma_0(s)\int_0^{\infty} d\xi^2\{1-\exp[-\chi(\xi,s)]\}. \quad (16)$$

The calculation of these cross sections requires specifying $\sigma_s(s)$ with a corresponding value of cutoff momenta $p_0\approx 2$ GeV/c [68].

In the energy range $10<\sqrt{s}<70$ GeV, where only soft parton interactions are important, the soft cross section $\sigma_s(s)$ is fixed by the data on total cross sections $\sigma_{\rm tot}(s)$ directly. In and above the S$p\bar{p}$S energy range $\sqrt{s}\geq 200$ GeV, a fixed $\sigma_s(s)=57$ mb and a minijet cutoff scale $p_0=2$ GeV/c, lead to the observed energy dependence of the cross sections and inclusive distributions. Between the two regions $70<\sqrt{s}<200$ GeV, a smooth extrapolation for $\sigma_s(s)$ is used.

In HIJING, a nucleus-nucleus collision is decomposed into a sequence of binary collisions involving in general excited or wounded nucleons. Wounded nucleons are assumed to be $q-qq$ stringlike configurations that decay on a slow time scale compared to the collision time of the nuclei. In the FRITIOF scheme wounded nucleon interactions follow the same excitation law as the original hadrons. In the DPM scheme subsequent collisions essentially differ from the first since they are assumed to involve sea partons instead of valence ones. The HIJING model adopts a hybrid scheme, iterating string-string collisions as in FRITIOF but utilizing DPM-like distributions. In the SPS range the HIJING results for nuclear collisions are very similar to those of FRITIOF. However, HIJING provides an interpolation model between the nonperturbative beam jet fragmentation physics at intermediate CERN SPS energies and perturbative QCD minijet physics at the highest collider energies [Relativistic Heavy Ion Collider (RHIC) and LHC].

III. NUMERICAL RESULTS

A. Strangeness in proton-proton interaction

We used the program HIJING with default parameters: IHPR2(11)=1 gives the baryon production model with diquark-antidiquark pair production allowed, the initial diquark treated as a unit; IHPR2(12)=1, the decay of particles such as π^0, K_s^0, Λ, Σ, Ξ, and Ω is allowed; IHPR2(17)=1 gives a Gaussian distribution of transverse momenta of the sea quarks; IHPR2(8)=0, jet production is turned off for theoretical predictions denoted by HIJING; and IHPR2(8) =10, when jet production is turned on for theoretical predictions denoted by HIJING$^{(j)}$ for comparison.

In Table I the calculated average multiplicities of particles at $E_{\rm lab}=200$ GeV in proton-proton (pp) interactions are compared to data. The theoretical values HIJING and HIJING$^{(j)}$ are obtained for 10^5 generated events and in a full phase space. The values HIJING$^{(j)}$ include the very small possibility of minijet production at these low SPS energies. The experimental data are taken from Gazdzicki and Hansen [15].

The small kaon to pion ratio is due to the suppressed strangeness production basic to string fragmentation. Positive pions and kaons are more abundant than the negative

TABLE I. Particle multiplicities for pp interaction at 200 GeV are compared with data from Gazdzicki and Hansen [15].

pp	Expt. data	HIJING	HIJING$^{(j)}$
$\langle\pi^-\rangle$	2.62±0.06	2.61	2.65
$\langle\pi^+\rangle$	3.22±0.12	3.18	3.23
$\langle\pi^0\rangle$	3.34±0.24	3.27	3.27
$\langle h^-\rangle$	2.86±0.05	2.99	3.03
$\langle K^+\rangle$	0.28±0.06	0.32	0.32
$\langle K^-\rangle$	0.18±0.05	0.24	0.25
$\langle\Lambda+\Sigma^0\rangle$	0.096±0.015	0.16	0.165
$\langle\bar{\Lambda}+\bar{\Sigma}^0\rangle$	0.013±0.01	0.03	0.037
$\langle K_s^0\rangle$	0.17±0.01	0.26	0.27
$\langle p\rangle$	1.34±0.15	1.43	1.45
$\langle\bar{p}\rangle$	0.05±0.02	0.11	0.12

ones due to charge conservation. We note that the *integrated* multiplicities for neutral strange particles $\langle\Lambda\rangle$, $\langle\bar{\Lambda}\rangle$, and $\langle K_s^0\rangle$ are reproduced at the level of three standard deviations for pp interactions at 200 GeV. However, the values for $\langle\bar{p}\rangle$ and $\langle\bar{\Lambda}\rangle$ are significantly over predicted by the model. This is important since as we shall see the $\bar{\Lambda}$ in S+S is significantly underestimated by HIJING.

For completeness we include a comparison of hadron yields at collider energies $\sqrt{s}=546$ GeV (S$p\bar{p}$S energies) for $\bar{p}p$ interactions, where minijet production plays a much more important role. From different collider experiments Alner *et al.* (UA5 Collaboration) [86] attempted to piece together a picture of the composition of a typical soft event at the S$p\bar{p}$S [87]. The measurements were made in various different kinematic regions and have been extrapolated in the full transverse momenta (p_T) and rapidity range for comparison as described in Ref. [86]. The experimental data are compared to theoretical values obtained with HIJING$^{(j)}$ in Table II. It was stressed by Ward [87] that the data show a substantial excess of photons compared to the mean $\pi^+ + \pi^-$. A gluon Cerenkov radiation emission in hadronic collisions was suggested as a possible explanation of such enhancement [88]. Our calculation rules out such a hypothesis. Taking into account decay from resonances and direct γ production, good agreement is found within the experimental errors.

TABLE II. Particle composition of $p+\bar{p}$ interactions at 540 GeV in cm.

Particle type	$\langle n\rangle$	Expt. data	HIJING$^{(j)}$
All charged	29.4±0.3	[86]	28.2
$K^0+\bar{K}^0$	2.24±0.16	[86]	1.98
$K^+ + K^-$	2.24±0.16	[86]	2.06
$p+\bar{p}$	1.45±0.15	[87]	1.55
$\Lambda+\bar{\Lambda}$	0.53±0.11	[86]	0.50
$\Sigma^+ + \Sigma^- + \bar{\Sigma}^+ + \bar{\Sigma}^-$	0.27±0.06	[87]	0.23
Ξ^-	0.04±0.01	[86]	0.037
γ	33±3	[86]	29.02
$\pi^+ + \pi^-$	23.9±0.4	[86]	23.29
K_s^0	1.1±0.1	[86]	0.99
π^0	11.0±0.4	[87]	13.36

The experimental ratio $K^+/\pi^+ = 0.095 \pm 0.009$ is also reproduced by the HIJING$^{(j)}$ model (0.099). We note that a detailed study of the ratios of invariant cross sections of kaons to those of pions as a function of transverse momenta in the central region was presented in [67].

In the following plots the kinematic variables used to describe single particle properties are the transverse momentum p_T and the rapidity y defined as usual as

$$y = \frac{1}{2}\ln\frac{E+p_3}{E-p_3} = \ln\frac{E+p_3}{m_T} \tag{17}$$

with E, p_3, and m_T being energy, longitudinal momentum, and transverse mass $m_T = \sqrt{m_0^2 + p_T^2}$ with m_0 being the particle rest mass.

In Figs. 1(a), 2(a), 3(a), and 4(a), we show rapidity and transverse momentum distributions for Λ's [Figs. 1(a) and 3(a)] and K_s^0's [Figs. 2(a) and 4(a)] produced in pp scattering at 200 GeV. The theoretical histograms obtained with HIJING (solid) and VENUS4.13 (dashed) are compared with experimental data taken from Jaeger *et al.* [89]. The HIJING spectra for Λ and K_s^0 are close to the data at midrapidity [89], although the dip in the K_s^0 yield at midrapidity and the Λ peak in the fragmentation regions are not well reproduced (see also Ref. [60]). Unfortunately, more precise data are not available in pp interactions and those features could reflect experimental acceptance cuts. Similarly, no detailed $\bar{\Lambda}$ spectra are as yet available in pp.

In comparison with VENUS (taking 10^4 events) we note that this version seems to overpredict the $pp \to \Lambda^0$ rapidity density at midrapidity by 50–100 % in Fig. 1(a), even though the rapidity integrated transverse momentum distribution in Fig. 3(a) seems closer to the data. The K_s^0 yields in Figs. 3(a) and 6(a) are similar to those of HIJING with the dip structure in the data absent.

The very sparse data base on pp strangeness production at SPS energies should be expanded in the future to improve the test of dynamical models before they are applied to the more complex nuclear collision case. Without $\bar{\Lambda}$ spectra in pp, for example, the need for the new dynamical mechanisms in that channel cannot be confirmed.

B. Multiplicities in pA and AA collisions

In this section, we compare strange particle production in the HIJING and VENUS models to pA and AA data. Again we limit the study to Λ, $\bar{\Lambda}$, and K_s^0 to compare with recent data from Alber *et al.* [18]. First we consider the average integrated multiplicities for negative hadrons $\langle h^-\rangle$, negative pions $\langle\pi^-\rangle$, and neutral strange particles $\langle K_s^0\rangle$, $\langle\Lambda\rangle$, and $\langle\bar{\Lambda}\rangle$ in pp, pS, pAg, and pAu (minimum bias collisions) and SS, SAg, and SAu (central collisions) at 200A GeV. The default parameters of HIJING were used without minijet production [IHPR2(8)=0]. The number of Monte Carlo generated events was 10^5 for HIJING and 10^4 for VENUS for pp and pA interactions, and 5×10^3 for SS and 10^3 for S+Ag, W, Au and PbPb collisions.

The mean multiplicities are compared in Table III (for pp and pA interactions) and in Table IV (for AA interactions)

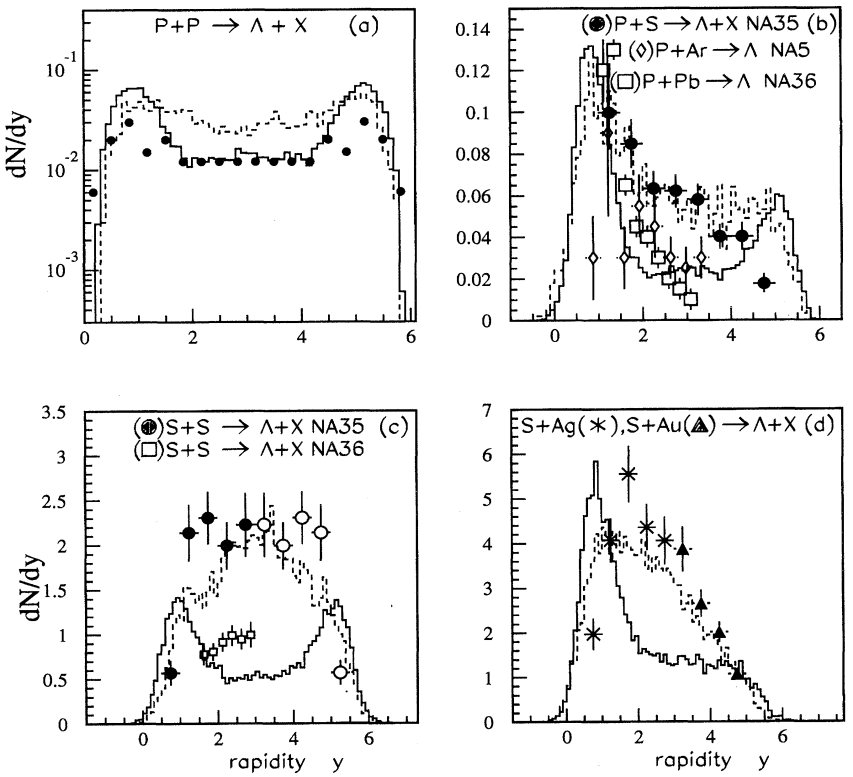

FIG. 1. Rapidity distributions of Λ^0 produced in pp interactions at 200 GeV (a). The data for pp (black small circles) are from Jaeger *et al.* [89]. Rapidity distributions of Λ^0 produced in minimum bias pS (b) and central SS (c), SAg (d) and SAu (d) collisions at 200*A* GeV. HIJING and VENUS results are shown by solid and dashed histograms, respectively (for pp, pS, SS, and SAu). The new NA35 data (pS, SS, full circles; SAg, stars; SAu, full triangles) are from Alber *et al.* [18]. The open circles show the distributions for SS collisions reflected at $y_{\rm lab}=3.0$. In (b), earlier NA5 data on $p+$Ar (open diamonds) from Ref. [14] and preliminary data on $p+$Pb (open squares) from NA36 [19,26] are shown for comparison. (c) NA36 data on S+S (open squares) are also shown for comparison.

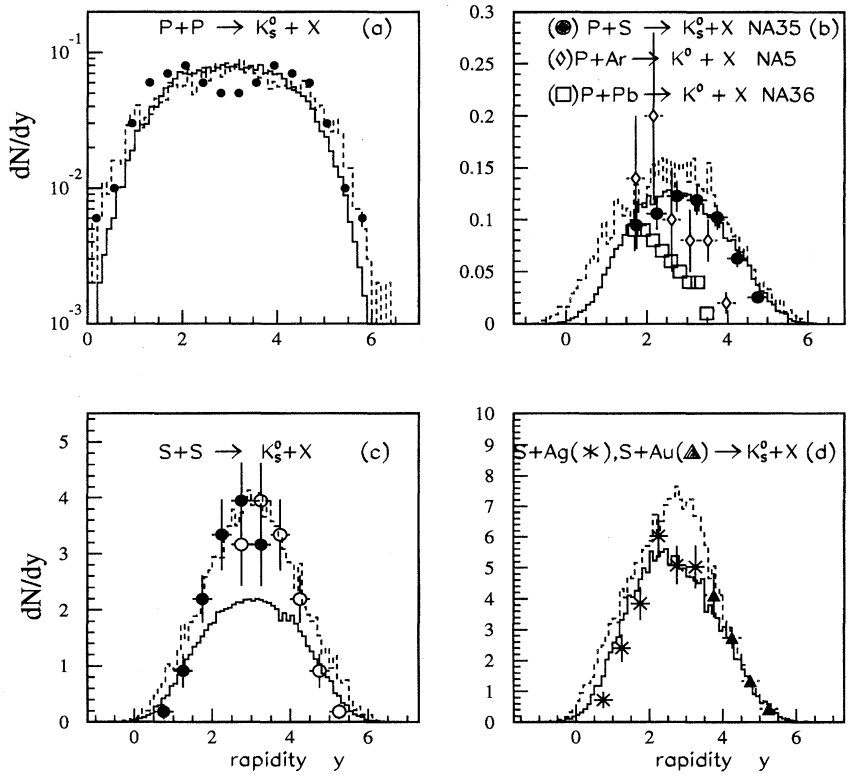

FIG. 2. As in Fig. 1 but for K_s^0 particles.

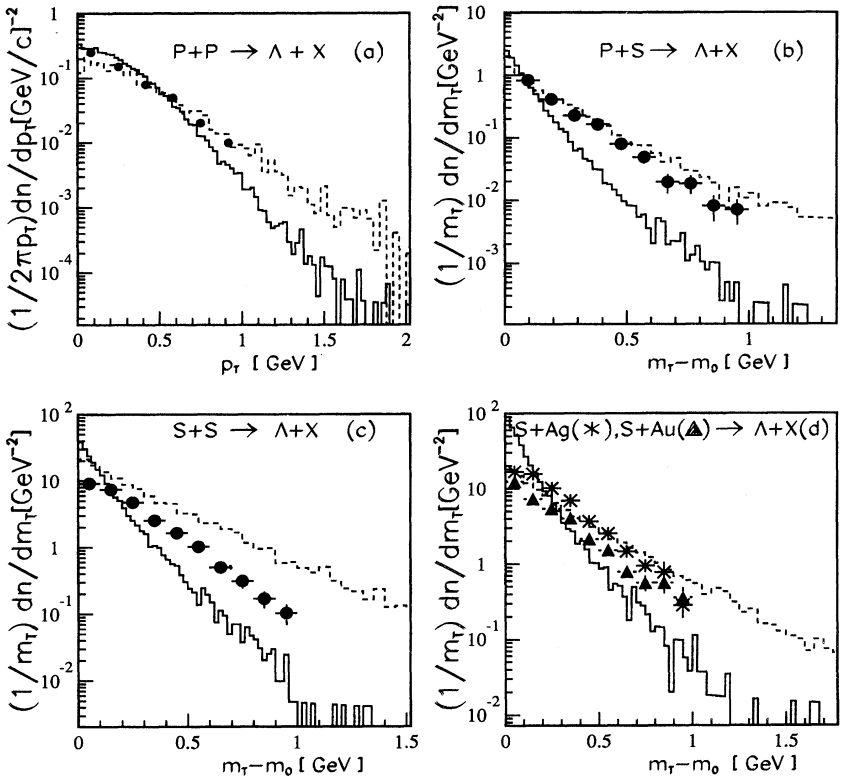

FIG. 3. Transverse momentum distributions of Λ^0 produced in pp interactions at 200A GeV (a). The data (black small circles) for pp interactions are from Jaeger *et al.* [89]. Transverse kinetic energy distributions of Λ^0 produced in minimum bias pS (b) and central SS (c), SAg (d), and SAu (d) collisions at 200A GeV. HIJING and VENUS results are shown by solid and dashed histograms, respectively (for pp, pS, SS, and SAu). The NA35 data (pS, SS, full circles; SAg stars; SAu, full triangles) are from Alber *et al.* [18].

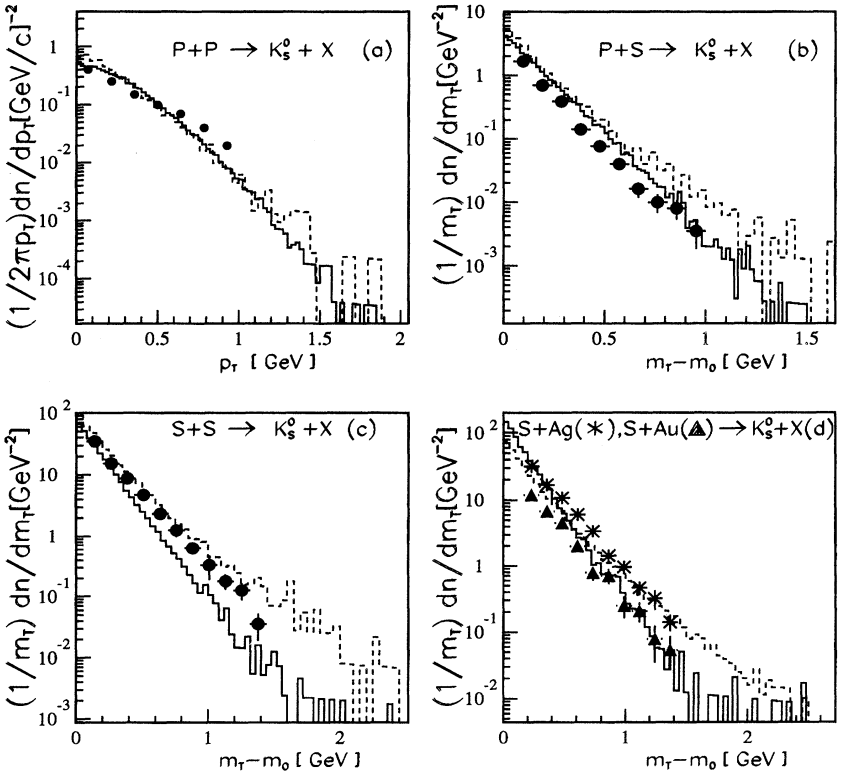

FIG. 4. As in Fig. 3, but for K^0_s particles.

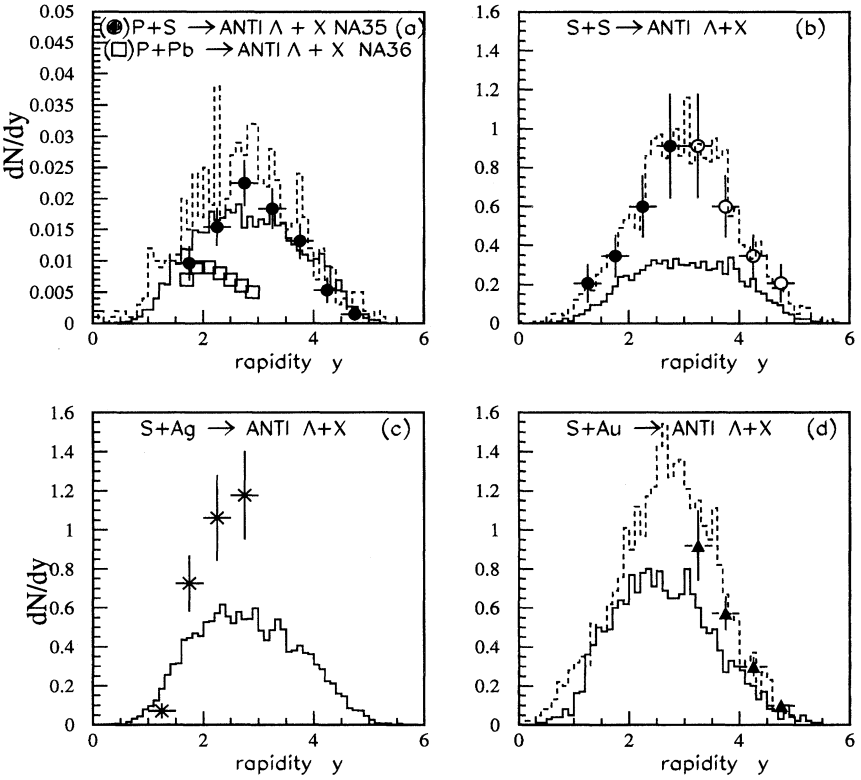

FIG. 5. Rapidity distributions of $\bar{\Lambda}$ produced in minimum bias pS (a) and central SS (b), SAg (c) and SAu (d) collisions at 200A GeV. Solid and dashed histograms are as in Fig. 1. The NA35 data (pS, SS, full circles; SAg, stars; SAu, full triangles) are from Alber *et al.* [18]. The open circles show the distributions for SS collisions reflected at $y_{\rm lab}=3.0$. In (a), the open squares correspond to preliminary $p+$Pb data from NA36 [19,26].

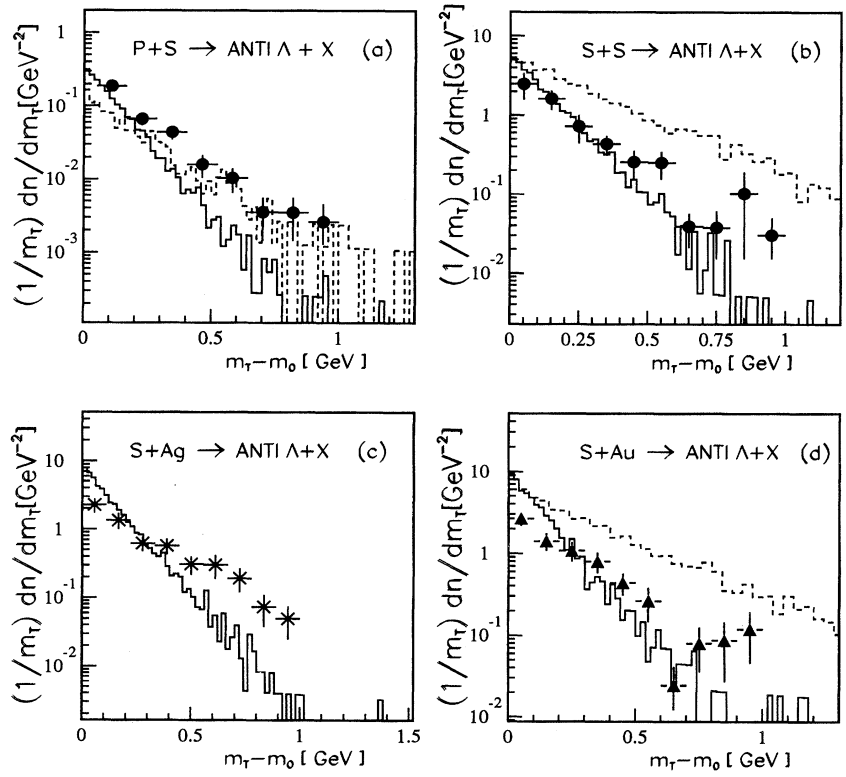

FIG. 6. Transverse kinetic energy distributions for $\bar{\Lambda}$ particles produced in minimum bias pS (a) and central SS (b), SAg (c) and SAu (d) collisions at 200 GeV per nucleon. Solid and dashed histograms are as in Fig. 3. The experimental data (pS, SS, full circles; SAg, stars; SAu, full triangles) are from Alber *et al.* [18].

TABLE III. Average multiplicities for negatively charged hadrons and neutral strange hadrons in pp and pA interactions. HIJING and VENUS model results are compared with other recent estimates using RQMD, QGSM, and DPM and with data from Alber *et al.* [18].

Reaction		$\langle h^- \rangle$	$\langle \Lambda \rangle$	$\langle \bar{\Lambda} \rangle$	$\langle K_s^0 \rangle$
$p+p$	data	2.85±0.03	0.096±0.015	0.013±0.005	0.17±0.01
	HIJING	2.99	0.16	0.030	0.26
	VENUS	2.79	0.181	0.033	0.27
	RQMD	2.59	0.11		0.21
	QGSM	2.85	0.15	0.015	0.21
	DPM[1]	3.52	0.155	0.024	0.18
	DPM[2]	3.52	0.155	0.024	0.18
$p+$S	data	5.7±0.2	0.28±0.03	0.049±0.006	0.38±0.05
min. bias	HIJING	4.83	0.255	0.046	0.400
	VENUS	5.40	0.340	0.065	0.510
	QGSM	5.87	0.240	0.023	0.340
	DPM[1]	5.53	0.300	0.043	0.360
	DPM[2]	5.54	0.32	0.060	0.360
$p+$Ag	data	6.2±0.2	0.37±0.06	0.05±0.02	0.525±0.07
min. bias	HIJING	6.28	0.34	0.054	0.505
$p+$Au	data	9.6±0.2			
central	HIJING	11.25	0.67	0.090	0.88

with experimental data from Alber *et al.* [18]. Note that, while the HIJING model describes well the integrated neutral strange particle multiplicities (except for $\langle \bar{\Lambda} \rangle$) in pp and pA interactions, there is a large discrepancy already for the light ion S+S reaction.

It is worthwhile to mention that theoretical calculations have been done for pA a "minimum bias" collisions and the experimental data are for the events with charged particle multiplicity greater than 5, which contain a significant fraction (about 90%) of the "minimum bias" events [18].

In Tables III and IV the data are compared also with other theoretical values obtained in some models VENUS (as computed here), RQMD [18], QGSM [59,18], and DPM. The theoretical values DPM[1] are from the Mohring *et al.* [49] version of the DPM which include additionally (qq)-$(\bar{q}\bar{q})$ production from the sea into the chain formation process and the values DPM[2] are from the Mohring *et al.* [50] version of the DPM which includes chain fusion as a mechanism to explain the anomalous antihyperon production.

TABLE IV. Average multiplicities for negatively charged hadrons and neutral strange hadrons in AA interactions. HIJING and VENUS model results are compared with other recent estimates using RQMD, QGSM, and DPM and with data from Alber *et al.* [18].

Reaction		$\langle h^- \rangle$	$\langle \Lambda \rangle$	$\langle \bar{\Lambda} \rangle$	$\langle K_s^0 \rangle$
S+S	data	95±5	9.4±1.0	2.2±0.4	10.5±1.7
	HIJING	88.8	4.58	0.86	7.23
central	VENUS	94.06	8.20	2.26	11.94
	RQMD	110.2	7.76		10.0
	QGSM	120.0	4.70	0.35	7.0
	DPM[1]	109.8	6.83	0.80	10.6
	DPM[2]	107.0	7.18	1.57	10.24
S+Ag	data	160±8	15.2±1.2	2.6±0.3	15.5±1.5
	HIJING	164.35	8.61	1.48	13.20
central	RQMD	192.3	13.4		18.30
	DPM[1]	195.0	13.3	1.45	19.40
	DPM[2]	186.90	14.06	3.65	15.73
S+Au	HIJING	213.2	11.3	1.81	16.55
central	VENUS	201.6	14.0	3.01	21.52
S+W	HIJING	210.0	10.64	1.71	16.05
central					
Pb+Pb	HIJING	725.15	36.44	5.93	54.86
central					

TABLE V. The mean multiplicities of negative pions and E_S ratios (see the text for definition) for nuclear collisions at 200A GeV. The data are from Alber *et al.* [18] and the NN data are from Gazdzicki and Hansen [15].

Reaction		$\langle \pi^- \rangle$	$\langle E_S \rangle$
$p+p$	data	2.62±0.06	
	HIJING	2.61	0.153
$N+N$	data	3.06±0.08	0.100±0.01
	HIJING	2.89	0.140
$p+$S	data	5.26±0.13	0.086±0.008
min. bias	HIJING	4.3	0.144
$p+$Ag	data	6.4±0.11	0.108±0.009
min. bias	HIJING	5.59	0.141
$p+$Au	data	9.3±0.2	0.073±0.015
central	HIJING	10.22	0.136
S+S	data	88±5	0.183±0.012
central	HIJING	79.6	0.140
S+Ag	data	149±8	0.173±0.017
central	HIJING	147.8	0.138

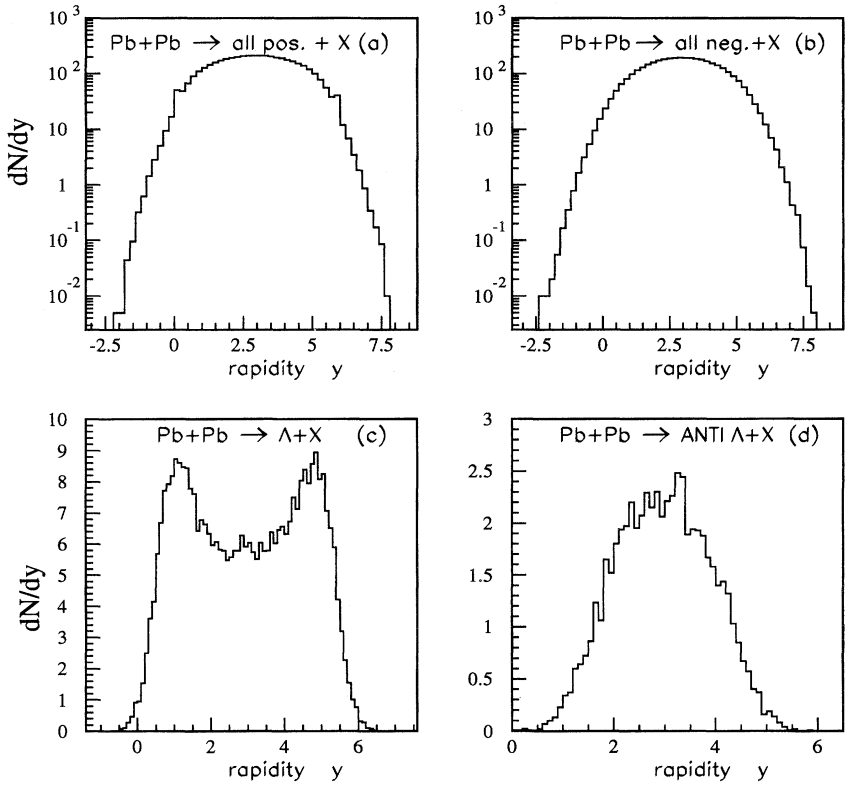

FIG. 7. Predicted rapidity distributions for central ($b=0-1$ fm) PbPb collisions at 170*A* GeV with the HIJING model for all positive charges (a), all negative charges (b), Λ (c), and $\bar{\Lambda}$ (d).

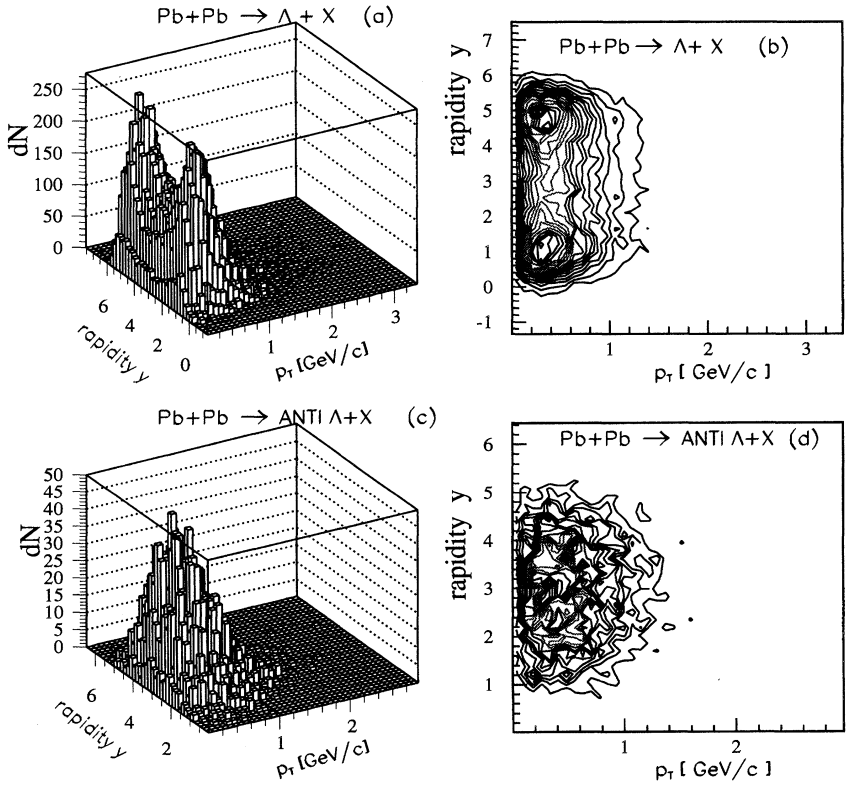

FIG. 8. Unnormalized rapidity y and transverse momentum p_T distributions for Λ (a) and (b) and $\bar{\Lambda}$ (c) and (d) for central PbPb at 170*A* GeV from HIJING.

Alber *et al.* [18] have considered that the total production of strangeness should be treated in a model independent way using all available experimental information for ratio E_S expressed as

$$E_S=\frac{\langle\Lambda\rangle+4\langle K_s^0\rangle}{3\langle\pi^-\rangle}\ . \tag{18}$$

We have calculated this ratio in the HIJING approach for the above interactions and the corresponding numerical predictions are shown in Table V. We note that there is much less discrepancy between HIJING and the data for this particular ratio. We conclude from this that such a ratio is insensitive to the underlying physics and therefore should NOT be used for any further tests of models. This ratio hides very effectively the gross deficiencies of the HIJING model in SS reactions pointed out later in the comparison to the rapidity and transverse momentum distributions. We include Table V only to prove the futility of studying the systematics of such ratios in the search for novel dynamics in nuclear collisions.

C. Single inclusive distributions for neutral strange particles in pA and AA

The main results of the present study are contained in Figs. 1–6. Figure 1 is our most important result revealing the systematics of Λ enhancement from (a) pp to (d) SAu. In part (a) the pp data at midrapidity are seen to be well reproduced by HIJING. However, the new minimum bias pS data [18] in Fig. 1(b) clearly show a factor of 2–3 discrepancy with respect to the linear extrapolation from pp as performed by HIJING. The effect of double string fragmentation and final state cascading, as modeled with VENUS, is seen, on the other hand, to account for the observed Λ enhancement. We note, however, that in pp VENUS overpredicts the Λ yield at midrapidity. Some fraction of the agreement in pS with VENUS may be due to this effect. The overprediction of midrapidity Λ's in pp by VENUS was shown in Fig. 10.20(b) of Ref. [60], but was not emphasized there. If both the pp and pS data on Λ production are correct, then the most striking increase of hyperon production therefore occurs between pp and pS reactions.

The strangeness enhancement in minimum bias $p+$S is striking because the number of target nucleons struck by the incident proton is on the average only 2. The step from single $p+p$ to triple $p+p+p$ reactions therefore apparently leads a substantial enhancement of midrapidity Λ's which obviously cannot have anything to do with equilibrium physics.

In central S+S reactions shown in Fig. 1(c), the discrepancy relative to HIJING grows by another factor of 2. We note that the new data [18] shown here have increased substantially relative to earlier data [7,8] due to inclusion of lower transverse momentum regions and Λ's originating from the decay of Σ and Ξ in the analysis. Including these decay channels, VENUS is seen to reproduce the new data as well. We note that with RQMD the excess Λ's are also reproduced with the introduction of rope formation (see Table IV). For heavier targets Ag and Au in Fig. 1(d), the discrepancy relative to HIJING is in fact less dramatic than in S+S.

In central S+S, on the average each projectile nucleon interacts with only two target nucleons, but each target nucleon also interacts with two projectile ones. In effect, then, S+S reactions probe strangeness production in four-nucleon interactions $p+p+p+p\rightarrow\Lambda+X$. Such reactions appear to be approximately four times as efficient in producing midrapidity Λ's as the two-nucleon interactions in part (a). Our main conclusion therefore is that strangeness enhancement is a nonequilibrium dynamical effect clearly revealed in the lightest ion interactions.

Further support for this conclusion is shown in Figs. 3(a)–3(c) where the transverse momentum distributions are compared. We see that there is an enhancement of the Λ transverse momentum relative to pp in pS. Comparing to VENUS we can interpret Fig. 3(b) as evidence that the enhanced transverse momentum of Λ in pS is due to cascading. The discrepancy in Fig. 3(c) between VENUS and the data in SS may be due to the rapidity cuts in the data, which we have not included in the calculated spectra. In all cases the deficiency of the linear extrapolation via the HIJING model is clearly evident. For heavier targets, S+Ag, Au, the transverse momentum distribution predicted by VENUS is close to the data.

The same general conclusion emerges from the systematics of $\bar{\Lambda}$ and K_s^0 production s in Figs. 5 and 2 and in Figs. 6 and 4, respectively. In Fig. 5(a), the agreement between HIJING and VENUS and the data on the $p+\mathrm{S}\rightarrow\bar{\Lambda}$ must be viewed with caution since, as shown in Table III, both models overpredict the integrated $\bar{\Lambda}$ multiplicity by a factor 2–3. Given the absence of more detailed rapidity and transverse momentum distributions for $\bar{\Lambda}$, it is not possible to determine whether the pp and pA data are compatible. However, at least the step from pS to SS in Fig. 5(b) indicates a possible factor of 2 enhancement of $\bar{\Lambda}$, similar to the comparison of Figs. 1(b) and 1(c) for Λ. As in the case of Λ production, there appears to be no further $\bar{\Lambda}$ enhancement from SS to SAu. As regards the transverse momentum distributions in Fig. 6, we note that as in Fig. 3 the $\bar{\Lambda}$ emerge with higher $p_\perp$ in pS than in pp in accord with the VENUS model. We note that in Figs. 6(c) and 6(d) the norm theoretical curves are obtained by integrating over the full rapidity interval, while the norm data are limited to a smaller domain as shown in Figs. 5(b) and 5(c).

In the case of K_s^0 production in Figs. 2 and 4 the same general trends are seen but in a less dramatic form.

We conclude that the new data indicate that the origin of strangeness enhancement in heavy ion collisions may be traced back to nonconventional and necessarily nonequilibrium dynamical effects that arise in collisions of three or more nucleons. However, this conclusion is forced upon us by the sytematics of the new light ion data on $p+$S and S+S reported in [18]. As shown in Figs. 1(b), 5(a), and 2(b), those systematics, especially in pA, differ considerably from the trends of earlier NA5 data [14] and preliminary NA36 data [19–26]. Those data for *heavier* target nuclei indicate substantially less enhancement of midrapidity Λ, $\bar{\Lambda}$, and K_s^0 than do the NA35 data on $p+$S. Part of the difference between these data sets may be due to different acceptance cuts and the inclusion or rejection of fragments from decay of higher mass hyperons. Obviously, the difference between these data sets must be resolved. Until then, the NA36 data must be regarded as an important caveat on our conclusions.

For completeness we show also in Fig. 7 the linear extrapolations of HIJING to Pb+Pb at 170*A* GeV for all positive [Fig. 7(a)] and all negative charges [Fig. 7(b)], for Λ [Fig. 7(c)], and for $\bar{\Lambda}$ [Fig. 7(d)]. It will be interesting to compare these extrapolations with upcoming data to test if the strangeness enhancement increases from SS to PbPb.

We include the two-dimensional distributions in Fig. 8 to emphasize that strangeness enhancement analyses restricted to narrow rapidity and transverse momentum cuts, especially with simplistic fireball models, may completely miss the global nonequilibrium character of the data.

IV. CONCLUSIONS

In this paper we performed a systematic analysis of strange particle production in pp, pA, and AA collisions at SPS CERN energies using the HIJING and VENUS models. The most surprising result is that the breakdown of the linear extrapolation from pp data to nucleus-nucleus in the strangeness channel already occurs in minimum bias pS. The apparent enhancement of Λ, $\bar{\Lambda}$, and K_s^0 at midrapidities in pS reactions by a factor of 2 indicates that the mechanism for strangeness enhancement in heavier ion collisions must be associated with nonequilibrium dynamics involving multiparticle production and not with equilibrium quark-gluon fireballs. In minimum bias pS one projectile nucleon interacts on the average with only two target ones. The data [18] on pS therefore indicate the existence of new dynamical mechanisms for strangeness production that become operative in $p+p+p$ collisions. The new data [18] on central S+S show another factor of 2 enhancement of strangeness production relative to pS. This light ion reaction basically probes multiparticle production in $p+p+p+p$. The strangeness enhancement in heavier target systems apparently saturates at the S+S level. We also showed that traditional analysis of strangeness enhancement in terms of ratios of integrated multiplicities is very ineffective since those ratios hide well defects of the detailed rapidity and transverse momentum distributions predicted by models.

The agreement with VENUS and RQMD results suggests color rope formation as a possible mechanism. However, to clarify the new physics much better quality data on elementary $p+p$ as well as on other light ion $p+\alpha$, C, S and $\alpha+\alpha$, C, S reactions will be needed. Especially, the discrepancy between NA35 and NA36 data must be resolved. Only then can strangeness enhancement systematics be used meaningfully in the search for signatures of quark-gluon plasma formation in future experiments with Au+Au and Pb+Pb.

ACKNOWLEDGMENTS

We are grateful to Klaus Werner for providing the source code of VENUS. One of the authors (V.T.P.) would like to express his gratitude to Professor C. Voci for his kind invitation and acknowledges financial support from INFN-Sezione di Padova, Italy where this work was initiated. V.T.P. is also indebted to Professor E. Quercigh for his kind hospitality at CERN (May 1994), and for very useful discussions. Finally, V.T.P. gratefully acknowledges partial financial support from the Romanian Soros Foundation for Open Society Bucharest, Romania. This work was supported by the Director, Office of Energy Research, Division of Nuclear Physics of the Office of High Energy and Nuclear Physics of the U.S. Department of Energy under Contract No. DE-FG02-93ER40764.

[1] *Quark Matter '93,* Proceedings of the Tenth International Conference on Ultra-Relativistic Nucleus-Nucleus Collisions, Borlange, Sweden, 1993, edited by E. Stenlund, H. A. Gustafsson, A. Oskarsson, and I. Otterlund [Nucl. Phys. **A566**, 1c (1994)].
[2] *Proceedings of a NATO Advanced Study Institute on Particle Production in Highly Excited Matter,* Il Ciocco, Italy, 1992, edited by Hans H. Gutbrod and Johann Rafelski (Plenum Press, New York, 1993).
[3] P. Koch, B. Muller, and J. Rafelski, Phys. Rep. **142**, 167 (1986).
[4] E. Quercigh, in *Proceedings of a NATO Advanced Study Institute on Particle Production in Highly Excited Matter* [2], p. 499.
[5] J. Letessier, J. Rafelski, and Ahmed Tounsi, Phys. Lett. B **323**, 393 (1994); Report No. PAR-LPTHE-92-27-REV, 1992 (unpublished).
[6] E. Quercigh, Nucl. Phys. **A566**, 321c (1994).
[7] J. Bartke *et al.*, Z. Phys. C **48**, 191 (1990).
[8] R. Stock *et al.*, Nucl. Phys. A **525**, 221c (1991).
[9] P. Seyboth *et al.*, Nucl. Phys. A **544**, 293c (1992).
[10] M. Kowalski *et al.*, Nucl. Phys. A **544**, 609c (1992).
[11] H. Bialkowska *et al.*, Z. Phys. C **55**, 491 (1992).
[12] J. Baechler *et al.*, Z. Phys. C **58**, 367 (1993).
[13] A. Bamberger *et al.*, Z. Phys. C **43**, 25 (1989).
[14] I. Derado *et al.*, Z. Phys. C **50**, 31 (1991).
[15] M. Gazdzicki and O. Hansen, Nucl. Phys. **A528**, 754 (1991).
[16] M. Gazdzicki *et al.*, Nucl. Phys. **A566**, 503c (1994).
[17] H. Strobele *et al.*, Nucl. Phys. A **525**, 59c (1991).
[18] T. Alber *et al.*, Z. Phys. C **64**, 195 (1994).
[19] E. Andersen *et al.*, Nucl. Phys. **A566**, 217c (1994).
[20] E. Andersen *et al.*, Nucl. Phys. **A566**, 487c (1994).
[21] D.E. Greiner *et al.*, Nucl. Phys. **A544**, 309c (1992).
[22] E. Anderson *et al.*, Nucl. Phys. **A553**, 817c (1993).
[23] E. Andersen *et al.*, Phys. Lett. B **294**, 127 (1992).
[24] E. Andersen *et al.*, Phys. Lett. B **316**, 603 (1993).
[25] E. Andersen *et al.*, Phys. Lett. B **327**, 433 (1944).
[26] NA36 Collaboration, D. Greiner *et al.*, LBL-36882, 1995 (unpublished).
[27] NA36 Collaboration, E. Judd, in Proceedings of the Eleventh International Conference on Ultra-Relativistic Nucleus-Nucleus Collisions, Monterey, 1995 [Nucl. Phys. A (in press)].
[28] S. Abatzis *et al.*, Nucl. Phys. **A566**, 225c (1994).
[29] F. Antinori *et al.*, Nucl. Phys. **A566**, 491c (1994).
[30] S. Abatzis *et al.*, Nucl. Phys. **A566**, 499c (1994).
[31] S. Abatzis *et al.*, Phys. Lett. B **244**, 130 (1990).
[32] S. Abatzis *et al.*, Phys. Lett. B **259**, 508 (1991).

[33] S. Abatzis *et al.*, Phys. Lett. B **270**, 123 (1991).
[34] S. Abatzis *et al.*, Nucl. Phys. **A525**, 445c (1991).
[35] J.B. Kinson *et al.*, Nucl. Phys. **A544**, 321c (1992).
[36] T. Akesson *et al.*, Z. Phys. C **53**, 183 (1992).
[37] M. Sarabura *et al.*, Nucl. Phys. **A544**, 125c (1992).
[38] M. Murray *et al.*, Nucl. Phys. **A566**, 515c (1994).
[39] T. Abbot *et al.*, Phys. Rev. D **45**, 3906 (1992).
[40] Y. Miake *et al.*, Nucl. Phys. **A525**, 231c (1991).
[41] T. Abbot *et al.*, Phys. Rev. C **47**, 1351 (1993).
[42] K.J. Foley *et al.*, Nucl. Phys. **A544**, 325c (1992).
[43] R.S. Longacre *et al.*, Nucl. Phys. **A566**, 167c (1994).
[44] Johana Stachel *et al.*, Nucl. Phys. **A566**, 183 (1994).
[45] J. Barette *et al.*, Z. Phys. C **59**, 211 (1993).
[46] G.E. Diebold *et al.*, Phys. Rev. C **48**, 2984 (1993).
[47] M.N. Namboodiri *et al.*, Nucl. Phys. **A566**, 443c (1994).
[48] A. Capella, U. Sukhatme, C.I. Tan, and J. Tran Thanh Van, Phys. Rep. **236**, 225 (1994).
[49] H.J. Mohring, J. Ranft, A. Capella, and J. Tran Thanh Van, Phys. Rev. D **47**, 4146 (1993).
[50] H.J. Mohring, J. Ranft, C. Merino, and C. Pajares, Phys. Rev. D **47**, 4142 (1993).
[51] J. Ranft and S. Ritter, Z. Phys. C **27**, 413 (1985).
[52] H.J. Mohring, J. Ranft, and S. Ritter, Z. Phys. C **27**, 419 (1985).
[53] H.J. Mohring and J. Ranft, Z. Phys. C **52**, 643 (1991).
[54] A. Capella, C. Merino, H.J. Mohring, J. Ranft, J. Tran Thanh Van, Nucl. Phys. **A525**, 493c (1991).
[55] A.B. Kaidalov, Sov. J. Nucl. Phys. **33**, 733 (1981).
[56] A.B. Kaidalov and O.I. Piskunova, Z. Phys. C **30**, 145 (1986).
[57] A.B. Kaidalov, Nucl. Phys. **A525**, 39c (1991).
[58] N.S. Amelin, E.F. Staubo, L.P. Csernai, V.D. Toneev, and K.K. Gudima, Phys. Rev. C **44**, 1541 (1991).
[59] N.S. Amelin, L.V. Bravina, L.P. Csernai, V.D. Toneev, K.K. Gudima, and S.Yu. Sivoklokov, Phys. Rev. C **47**, 2299 (1993).
[60] K. Werner, University of Heidelberg, Germany, Report No. HD-TVP-93-1, 1993; Phys. Rep. **232**, 87 (1993).
[61] B. Andersson, G. Gustafson, and B. Nilsson-Almqvist, Nucl. Phys. **B281**, 289 (1987).
[62] B. Nilsson-Almqvist and E. Stenlund, Comput. Phys. Commun. **43**, 387 (1987).
[63] M. Gyulassy, CERN Report No. TH-4794/87, 1987; in Proceedings of the International Conference on Intermediate Energy Nuclear Physics, Balatonfured, Hungary, 1987.
[64] Xin-Nian Wang and Miklos Gyulassy, Comput. Phys. Commun. **83**, 307 (1994).
[65] Xin-Nian Wang, Phys. Rev. D **43**, 104 (1991).
[66] Xin-Nian Wang and Miklos Gyulassy, Phys. Rev. D **44**, 3501 (1991).
[67] Xin-Nian Wang and Miklos Gyulassy, Phys. Rev. D **45**, 844 (1992).
[68] Xin-Nian Wang and Miklos Gyulassy, Phys. Rev. Lett. **68**, 1480 (1992).
[69] J. Aichelin, G. Peilert, A. Bohnet, A. Rosenhauer, H. Socker, and W. Greiner, Phys. Rev. C **37**, 2451 (1988).
[70] H. Sorge, H. Stocker, and W. Greiner, Nucl. Phys. **A498**, 567c (1989).
[71] H. Sorge, L.A. Winckelmann, H. Stocker, and W. Greiner, Z. Phys. C **49**, 85 (1993).
[72] H. Sorge, Los Alamos Report No. LA-UR-93-1103, 1993.
[73] H. Sorge, Nucl. Phys. **A566**, 633c (1994).
[74] H. Sorge, Phys. Rev. C **49**, 1253 (1994).
[75] N.S. Amelin, H. Stocker, W. Greiner, N. Armesto, M.A. Braun, and C. Pajares, Santiago University Report No. US-FT/1-94, 1994 [Phys. Rev. C (submitted)].
[76] R. Folman and A. Shor, Nucl. Phys. **A566**, 917 (1994).
[77] K. Geiger and B. Mueller, Nucl. Phys. **B369**, 600 (1992).
[78] K. Geiger, Phys. Rev. D **47**, 133 (1993).
[79] K. Geiger, CERN Report No. CERN-TH-7313, 1994 [Phys. Rep. (submitted)].
[80] M. Braun and C. Pajares, Phys. Rev. D **47**, 114 (1993).
[81] C. Merino, C. Pajares, and J. Ranft, Phys. Lett. B **276**, 168 (1992).
[82] H. Mohring, J. Ranft, C. Merino, and C. Pajares, Phys. Rev. D **47**, 4142 (1993).
[83] T.S. Biro, H.B. Nielsen, and J. Knoll, Nucl. Phys. **B245**, 449 (1984).
[84] T. Sjostrand, Comput. Phys. Commun. **82**, 74 (1994).
[85] R.C. Hwa, Phys. Rev. D **37**, 1830 (1988).
[86] G.J. Alner *et al.*, Phys. Rep. **154**, 247 (1987).
[87] D.R. Ward, in *Proton Antiproton Collisions*, Advanced Series on Directions in High Energy Physics, Vol. 4, edited by G. Altarelli and L. Di Lella (World Scientific, Singapore, 1989), p. 85.
[88] I.M. Dremin, Sov. J. Nucl. Phys. **33**, 726 (1981).
[89] K. Jaeger *et al.*, Phys. Rev. D **11**, 2405 (1975).